Optimal Partitioning for Spatiotemporal Coverage in a Drift Field ⋆

Efstathios Bakolas [a] and Panagiotis Tsiotras [b]

[a] *Department of Aerospace Engineering and Engineering Mechanics, The University of Texas at Austin, Austin, TX 78712-1221, USA*

[b] *School of Aerospace Engineering, Georgia Institute of Technology, Atlanta, GA 30332-0150, USA*

Abstract

We consider the problem of partitioning an area in the plane populated by a team of aerial/marine vehicles into a finite collection of non-overlapping sets. The sets of this partition are in an one-to-one correspondence with the vehicles under the following rule: Each point in the given set of the partition can be reached by the corresponding vehicle in this set faster than any other vehicle in the presence of a spatiotemporal drift field. Consequently, a Voronoi-like partition results, which encodes the proximity relations between the vehicles and arbitrary points in the plane with respect to the minimum time-to-go. The construction of this Voronoi-like partition is based on its interpretation as the intersection of a forest of the cost (minimum time-to-go) surfaces emanating from each generator with their common lower envelope. The characterization of each cost surface is achieved by means of an efficient expansion scheme of the level sets of the minimum time-to-go function, which utilizes, in turn, the structure of the optimal synthesis of the minimum-time problem without resorting to exhaustive numerical techniques, e.g., fast marching methods. We examine the topological characteristics of the partition by using control/system theoretic concepts and tools. The theoretical developments are illustrated with a number of numerical examples.

Key words: Autonomous agents, Zermelo Voronoi diagram, Zermelo navigation problem, spatiotemporal coverage, computational methods.

1 Introduction

One fundamental problem in the context of spatiotemporal processes is the so-called *coverage* problem, in which one is interested in characterizing a set of rules such that a given set of points, known as *generators* or *primitives*, act as nodes of a network, whose purpose is to provide service to nearby points [1]. In this work, we assume that each generator corresponds to the initial position of a service vehicle from a team of spatially distributed autonomous aerial/marine vehicles. If a request is issued at some point, then a vehicle is required to provide service to this point, provided that it can reach it faster than any other vehicle from the same team. It should be highlighted here that the emphasis of this work is the characterization of the optimal partitioning problem for coverage for a team of vehicles with prescribed initial positions, which is mainly an optimization problem. This optimization problem is different from the coverage control problem where the objective is to find the locations at which the vehicles should be steered at such that certain coverage-related objectives are achieved. The reader interested in the literature of coverage control for sensor and robotic network applications can refer, for example, to [2–9].

The previously introduced coverage problem can be naturally associated with a Voronoi-like (or generalized Voronoi) partitioning problem, in which the distance function that determines the proximity relations between the vehicles and arbitrary points in the plane is the minimum time-to-go. We assume that the motion of each vehicle is modeled by a single integrator traveling in the presence of a spatiotemporal drift field, which models, in turn, the effect of the local winds/currents on the vehicle's motion. Therefore, the minimum time-to-go is the "value" function of the classical minimum-time problem, namely the Zermelo Navigation Problem (ZNP) [10]. Owing to the presence of the spatiotemporal drift field, this value function depends explicitly on both the location of the vehicle along its ensuing path, as well as time. In our previous work [11], we have coined the term Zermelo-Voronoi Diagram (ZVD) to describe the solution of the Voronoi-like partitioning

⋆ This work has been supported in part by NSF (CMMI award 1160780). Corresponding author P. Tsiotras. Tel.: +1 404 894 9526; Fax: +1 404 894 2760.

Email addresses: ebakolas@gatech.edu (Efstathios Bakolas), tsiotras@gatech.edu (Panagiotis Tsiotras).

problem with respect to the minimum time-to-go/come of the ZNP in the special case of a time-varying, but spatially invariant, drift field. Some previous treatments of the ZVD problem with respect to the minimum time-to-come of the ZNP can be found in [12–14]. In particular, [12] deals with the ZVD for a constant drift field, whereas [13,14] deal with the same problem for a spatially varying, yet time-invariant, drift field. On the one hand, the approaches presented in [11,12] are based on the existence of a homeomorphism that maps the ZVD to the standard Voronoi diagram generated by the same point-set. The approaches presented in [11,12] fail, however, when the drift field is spatially varying. On the other hand, the purely computational techniques proposed in [13,14], which suffer from some of the standard pathogenies associated with the numerical solution of optimal control problems, fail to exploit the intrinsic connection between the partitioning problem and the well studied ZNP. In contradistinction with [13,14], our approach makes use of the particular structure of the optimal synthesis of the ZNP; something that allows us to set the theoretical foundations for a computationally tractable scheme for the characterization of the ZVD for drift fields that vary both spatially and temporally.

One of the notable features of the ZVD is that its proximity metric belongs to the class of anisotropic, that is, direction-dependent, generalized distance functions, for which, except from a few special classes of problems [15,16], no universally efficient algorithms have been reported in the literature (see, for example, [17,18] and references therein). In addition, the ZVD does not naturally fit into the framework of "abstract Voronoi diagrams" introduced in [19]. In particular, the techniques presented in [19], which are aimed at covering a large collection of generalized Voronoi partitioning problems, require that the proximity metric behaves necessarily as a "nice" distance function [1] ; something that is not the case in our problem. For example, the minimum time-to-go function of the ZNP may be discontinuous even for linear drift fields. Therefore, the ZVD problem requires an alternative approach, whose applicability is not limited to well-known, particular instances of generalized Voronoi partitioning problems.

The approach we adopt in this work is based on the interpretation of a generalized Voronoi partition as the projection of the intersection of a "forest" of cost surfaces emanating from each generator with their common lower envelope [20]. We focus on the problem of computing the minimum time-to-go surfaces, whereas the characterization of their common lower envelope follows from standard techniques from computational geometry [21–24]. The proposed scheme for the computation of the cost surfaces builds upon some key features of the optimal control synthesis of the ZNP, some of which can be found in the classical treatment of this problem by Carathéodory [25] (which is based on techniques from calculus of variations) and the more modern treatment by Jurdjevic [26] (which is based on optimal control theory).

One of the key advantages of our approach is that it does not resort to exhaustive numerical schemes as those presented in [13,14], which do not account for some well-known results regarding the structure of the optimal synthesis of the ZNP. In particular, the candidate minimum-time trajectories of the ZNP form an one-parameter family of curves [10,25,27], a fact we systematically exploit in our approach to significantly expedite the computation of the cost surfaces. In contrast with other techniques proposed in the recent literature for numerically solving the ZNP problem [28–30], which also exploit the structure of the solution of the ZNP to some extent, our technique explicitly accounts for 1) the existence of trajectories which correspond to the solution of the maximum-time (rather than the minimum-time) navigation problem, and 2) the existence of time instants at which an extremal trajectory of the ZNP loses optimality. Note that both of these two issues are typically observed when the drift field exceeds the control authority of the vehicle in the vicinity of the latter, a situation that is encountered quite often in our analysis. In addition, we examine the topological characteristics of the ZVD by utilizing system theoretic/control tools. Some of these topological features can shed light on questions regarding the complexity of the ZVD viewed as a data structure, a property that affects the computational and memory cost impacting the applicability of the ZVD in practice.

It should be emphasized that, in contrast with some of our previous work on Voronoi-like partitioning problems, where time serves as the proximity metric [11,31,32], the techniques presented in the current work may be applicable to similar partitioning problems with respect to different state-dependent metrics, such as the minimum fuel/control effort-to-go, after the necessary modifications have been applied. Thus the proposed partition with respect to time can pave the way for a more general framework for dealing with problems involving teams of spatially distributed vehicles than some of the currently available approaches, which are mostly based on standard Voronoi partitions [3,5–7,32].

The rest of the paper is organized as follows. Section 2 formulates the ZVD partitioning problem, whose solution is characterized in Section 3. Some fundamental topological properties of the resulting optimal partition are presented in Section 4. Numerical simulation results are presented in Section 5. Finally, Section 6 concludes the paper with a summary of remarks.

2 Problem Formulation

Consider a set of distinct points $\mathcal{P} := \{\mathsf{p}^i \in \mathbb{R}^2,\ i \in \mathcal{I}_n\}$ in the plane, where $\mathcal{I}_n := \{1, \ldots, n\}$ and $\mathsf{p}^i := [x^i_{\mathsf{p}},\ y^i_{\mathsf{p}}]^{\mathsf{T}}$. It is assumed that at each point $\mathsf{p}^i \in \mathcal{P}$ resides, at time $t = 0$, an aerial/marine vehicle, which we henceforth refer to as the i–th vehicle. The motion of the i–th vehicle is described by the following equation

$$\dot{\mathsf{x}}^i = u^i(t) + w(t, \mathsf{x}^i), \qquad \mathsf{x}^i(0) = \mathsf{p}^i, \qquad i \in \mathcal{I}_n, \quad (1)$$

[1] For the definition of a "nice" metric the reader is referred to Definition 1.2.12 of [19].

where $\mathsf{x}^i := [x^i,\ y^i]^\mathsf{T} \in \mathbb{R}^2$ and u^i is, respectively, the position vector and the control input of the i–th vehicle, and $w(t,\mathsf{x}^i)$ is the drift field induced by the local winds/currents. It is assumed that the set of admissible control inputs, denoted by $\mathcal{U}$, consists of all piecewise continuous functions taking values in the set $U := \{u \in \mathbb{R}^2 :\ |u| \leq 1\}$ (closed unit ball). Furthermore, for every fixed $\mathsf{x}^i \in \mathbb{R}^2$, the mapping $t \mapsto w(t,\mathsf{x}^i)$ is piecewise continuous, and, for every fixed $t \geq 0$, the mapping $\mathsf{x}^i \mapsto w(t,\mathsf{x}^i)$ is at least C^1.

To simplify the analysis and streamline the presentation, it will be henceforth assumed that the drift field satisfies the following growth condition

$$|w(t,\mathsf{x}^i)| \leq \gamma(t) + \psi(t)|\mathsf{x}^i|, \tag{2}$$

where the functions $t \mapsto \gamma(t)$ and $t \mapsto \psi(t)$ are piecewise continuous and nonnegative. A class of drift fields that trivially satisfy the condition (2) are time varying inhomogeneous linear drift fields given by

$$w(t,\mathsf{x}^i) = \nu(t) + \mathsf{A}(t)\mathsf{x}^i, \tag{3}$$

where $\mathsf{A}(t) \in \mathbb{R}^{2\times 2}$ and $\nu(t) \in \mathbb{R}^{2\times 1}$, for all $t \geq 0$.

We will assume that the drift field w is known to all the vehicles a priori based on available weather data. The previous assumption is standard in the classical literature of the ZNP [10,25,27,26] and will allow us to formulate the problem of steering the i–th vehicle to a prescribed terminal position in minimum time as a deterministic optimal control problem.

2.1 The Navigation Problem

Given a point $\mathsf{x} \in \mathbb{R}^2$, the objective of the i–th vehicle, starting from point $\mathsf{p}^i \in \mathcal{P}$ at time $t = 0$, is to reach the point x in minimum-time. We shall refer to this problem as the i–th Navigation Problem (i–th NP).

Problem 1 (i–th Navigation Problem) *Given* $\mathsf{x} \in \mathbb{R}^2$*, determine the control input* $u^i_* \in \mathcal{U}$*, such that*

(i) The trajectory $t \mapsto \mathsf{x}^i_*(t)$ *of the system described by Equation* (1) *generated by the control* u^i_* *satisfies the boundary conditions* $\mathsf{x}^i_*(0) = \mathsf{p}^i$, $\mathsf{x}^i_*(T_\mathsf{f}) = \mathsf{x}$.

(ii) The control u^i_* *minimizes the cost functional* $J(u^i) := T_\mathsf{f}$*, where* T_f *is the final time.*

Henceforth, we denote by $T_\mathsf{f}(\mathsf{x};\mathsf{p}^i)$ *the cost functional* J *evaluated at* $u = u^i_*$.

Remark 1 Note that Problem 1 is a special case of the ZNP, whose complete solution is presented in [10] and [25, pp. 239-247, pp. 370-373].

The first question we wish to address is related to the feasibility of the i–th NP. To this aim, we first introduce the *reachable set* [33] of the system (1) from p^i, at time $\tau \geq 0$ (also known as the *set of attainability* [34] or the *attainable set* [35]), $\mathfrak{R}_\tau(\mathsf{p}^i) := \bigcup_{u^i\in\mathcal{U}}\{\mathsf{x} \in \mathbb{R}^2 :\ \mathsf{x} = \mathsf{x}^i(\tau;\mathsf{p}^i,u^i)\}$, where $t \mapsto \mathsf{x}^i(t;\mathsf{p}^i,u^i)$ denotes the solution of Eq. (1) with initial condition $\mathsf{x}^i(0) = \mathsf{p}^i$ and control law u^i. The reachable set $\mathfrak{R}_\tau(\mathsf{p}^i)$ consists of all the points that the i–th vehicle can reach, starting from p^i at $t = 0$, after exactly τ units of time with the application of some admissible control input from $\mathcal{U}$. We will say that the pair (x^i, u^i), where $u^i \in \mathcal{U}$ and $t \mapsto \mathsf{x}^i(t)$ is the corresponding trajectory, defines an *admissible pair* of the i–th NP problem [35]. If, for a given $\mathsf{x} \in \mathbb{R}^2$, there exists $u^i \in \mathcal{U}$ such that $\mathsf{x} = \mathsf{x}^i(\tau;\mathsf{p}^i,u^i)$ for some $\tau \geq 0$, we will say that the i–th NP admits a *feasible solution*. In addition, we denote by $\mathfrak{R}(\mathsf{p}^i)$ the set of reachable states of the system (1) from p^i, where $\mathfrak{R}(\mathsf{p}^i) := \bigcup_{0\leq\tau<\infty}\mathfrak{R}_\tau(\mathsf{p}^i)$. Note that if $\mathsf{x} \in \mathfrak{R}(\mathsf{p}^i)$, then there exists a finite time $\tau \geq 0$ and an admissible control $u^i \in \mathcal{U}$ that will drive the system (1), starting from p^i at time $t = 0$, to x in finite time. An immediate consequence of the definition of the reachable set is that the i–th NP admits a feasible solution if and only if $\mathsf{x} \in \mathfrak{R}(\mathsf{p}^i)$. The situation is illustrated in Fig. 1. In particular, Fig. 1(a) illustrates the case when $\mathsf{x} \notin \mathfrak{R}(\mathsf{p}^i)$, and consequently the i–th NP is infeasible. Figure 1(b), on the other hand, illustrates the case when x is an interior point of $\mathfrak{R}(\mathsf{p}^i)$, which implies, in turn, that the i–th NP admits a feasible solution. The reachable set $\mathfrak{R}(\mathsf{p}^i)$ in both Figs. 1(a) and 1(b) is identified by the isochronous curves (blue curves) of the i–th NP problem, that is, the curves consisting of points that can be reached at the same time $t = \tau$, computed for different values of $\tau \geq 0$. The procedure for the computation of these curves will be explained later on.

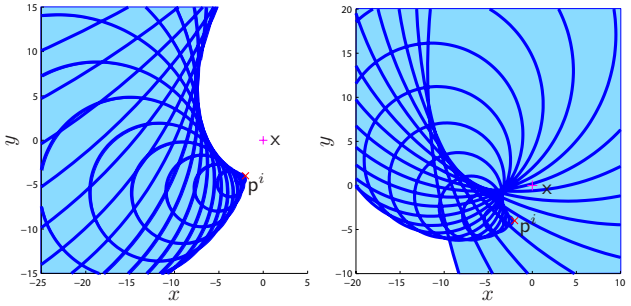

(a) Infeasible case: x belongs to the complement of $\mathfrak{R}(\mathsf{p}^i)$ (b) Solvable case: $\mathsf{x} \in \mathfrak{R}(\mathsf{p}^i)$

Fig. 1. The i–th NP admits a feasible solution if and only if the destination point x belongs to the reachable set $\mathfrak{R}(\mathsf{p}^i)$. The solid blue curves correspond to points that can be reached from p^i at the same time (isochronous curves).

In the subsequent analysis, we shall also consider sets consisting of points that can be reached from each $\mathsf{p}^i \in \mathcal{P}$ within a given time interval $[0,\tau]$, denoted by $\mathfrak{R}_{t\leq\tau}(\mathsf{p}^i) := \bigcup_{0\leq t\leq\tau}\mathfrak{R}_t(\mathsf{p}^i)$.

2.2 Existence of Optimal Solutions to the Navigation Problem

Next, we briefly examine the problem of existence of optimal solutions.

Proposition 1 *Let* $(t,\mathsf{x}^i) \mapsto w(t,\mathsf{x}^i)$ *be a drift field that satisfies* (2)*. Let both* $\gamma(t)$ *and* $\psi(t)$ *in* (2) *be bounded and suppose that* $\mathsf{x} \in \mathfrak{R}(\mathsf{p}^i)$*. Then the* i*–th NP has an optimal*

solution.

PROOF. From Filippov's Theorem on the existence of solutions of minimum-time problems [36, pp.310-317], it suffices to prove that there exists $k > 0$ such that $\langle \dot{\mathsf{x}}^i, \mathsf{x}^i \rangle \leq k(1 + |\mathsf{x}^i|^2)$. Since γ and ψ are bounded, there exist Γ, $\Psi > 0$ such that $|\gamma(t)| < \Gamma$ and $|\psi(t)| < \Psi$, for all $t \geq 0$. By virtue of the triangle and Cauchy-Schwartz inequalities and the fact that $|u^i| \leq 1$, it follows that $\langle \dot{\mathsf{x}}^i, \mathsf{x}^i \rangle \leq (|\psi(t)||\mathsf{x}^i| + |\gamma(t)| + |u^i|)|\mathsf{x}^i|$, which furthemore implies that $\langle \dot{\mathsf{x}}^i, \mathsf{x}^i \rangle \leq \Psi|\mathsf{x}^i|^2 + (\Gamma + 1)|\mathsf{x}^i|$. The result follows readily from the inequality $2|\mathsf{x}^i| \leq 1 + |\mathsf{x}^i|^2$. ■

2.3 The Partitioning Problem

Next, we formulate a Voronoi-like partitioning problem, in which the set of generators is the point-set $\mathcal{P}$ and the proximity metric is the minimum time-to-go function of the i–th NP. In addition, the set to be partitioned is taken to be the union of all the points that can be reached from at least one point from $\mathcal{P}$, denoted by $\mathfrak{R}(\mathcal{P}) := \bigcup_{i \in \mathcal{I}_n} \mathfrak{R}(\mathsf{p}^i)$.

Problem 2 *Let a collection of (distinct) points* $\mathcal{P} := \{\mathsf{p}^i \in \mathbb{R}^2 : i \in \mathcal{I}_n\}$ *be given, and let* $T_{\mathsf{f}}(\mathsf{x}; \mathsf{p}^i)$ *denote the minimum time required to drive the system described by Eq.* (1) *from* $\mathsf{p}^i \in \mathcal{P}$ *to* $\mathsf{x} \in \mathfrak{R}(\mathsf{p}^i)$*. Determine a partition* $\mathfrak{V} = \{\mathfrak{V}^i : i \in \mathcal{I}_n\}$ *of* $\mathfrak{R}(\mathcal{P})$ *such that*

(i) $\mathfrak{R}(\mathcal{P}) = \bigcup_{i \in \mathcal{I}_n} \mathfrak{V}^i$.
(ii) $\mathfrak{V}^i \subseteq \mathfrak{R}(\mathsf{p}^i)$.
(iii) $\mathsf{x} \in \mathfrak{V}^i$*, when* $T_{\mathsf{f}}(\mathsf{x}; \mathsf{p}^i) \leq T_{\mathsf{f}}(\mathsf{x}; \mathsf{p}^j)$ *for all* $i, j \in \mathcal{I}_n$.

The sets $\mathcal{P}$ and $\mathfrak{V}^i$, $i \in \mathcal{I}_n$, constitute, respectively, the set of the generators and the cells of the ZVD. We will say that two cells of the ZVD are neighboring if and only if they have a non-trivial intersection (not a singleton). Note that the condition ii) in the formulation of Problem 2 guarantees that $T_{\mathsf{f}}(\mathsf{x}; \mathsf{p}^i) < \infty$, for all $\mathsf{x} \in \mathfrak{V}^i$.

3 Characterization and Computation of the Zermelo-Voronoi Diagram

At this point, it is not clear whether the minimum time-to-go function of the i–th NP enjoys the nice properties, such as isotropy and convexity, that would allow us to associate Problem 2 with particular classes of generalized Voronoi partitioning problems, for which efficient computational methods exist in the literature [17,18]. Therefore, we need to adopt an alternative approach, suitable for more general classes of Voronoi-like partitioning problems.

3.1 Interpretation of the Voronoi-like Partition as the Tightest Lower Envelope of a Family of Generalized Parametric Surfaces

Let $\mathcal{S}_i$ denote the cost surface associated with the minimum time-to-go function of the i–th NP, which is defined by $\mathcal{S}_i := \{(\mathsf{x}, z) : \mathsf{x} \in \mathfrak{R}(\mathsf{p}^i),\ z = T_{\mathsf{f}}(\mathsf{x}; \mathsf{p}^i)\}$. We say that the generalized parametric surface $\mathcal{S}_{\mathcal{P}} := \{(\mathsf{x}, z) : \mathsf{x} \in \mathfrak{R}(\mathcal{P}),\ z = \min_{i \in \mathcal{I}_n} T_{\mathsf{f}}(\mathsf{x}; \mathsf{p}^i)\}$ defines a *lower envelope* of the family of the generalized parametric surfaces $\mathcal{S}_i$.

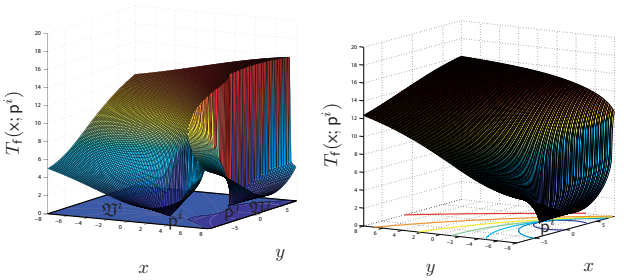

(a) The ZVD of two generators computed by projecting the intersection of the two cost surfaces with their common lower envelope.

(b) Computation of $\mathcal{S}_i$ by lifting the level sets $\ell_\tau(\mathsf{p}^i)$, for $\tau > 0$.

Fig. 2. The interpretation of (a) the cost surface $\mathcal{S}_i$ as the union of the lifted level sets $\Lambda_t(\mathsf{p}^i)$, for all $t \geq 0$, and (b) the ZVD as the projection of the intersection of all the cost surfaces with their common lower envelope.

Next, we describe a systematic way to compute the cells of the ZVD by first characterizing the intersection of each surface $\mathcal{S}_i$ with the lower envelope $\mathcal{S}_{\mathcal{P}}$. To this end, let us consider the following projection operator $\mathbf{P} : \mathfrak{R}(\mathcal{P}) \times [0, \infty) \mapsto \mathfrak{R}(\mathcal{P})$, such that $\mathbf{P}(\mathsf{x}, z) = \mathsf{x}$. The solution of Problem 2 can then be characterized by projecting the intersections of the lower envelope surface $\mathcal{S}_{\mathcal{P}}$ with each cost surface $\mathcal{S}_i$ on $\mathfrak{R}(\mathcal{P})$. The idea is to attach, by means of the projection operator $\mathbf{P}$, to each point $\mathsf{x} \in \mathfrak{R}(\mathcal{P})$ the integer $i \in \mathcal{I}_n$ for which $T_{\mathsf{f}}(\mathsf{x}; \mathsf{p}^i) \leq T_{\mathsf{f}}(\mathsf{x}; \mathsf{p}^j)$, for all $j \in \mathcal{I}_n \backslash \{i\}$. In particular, let $\mathfrak{I}(\mathsf{x}) := \arg\min_{i \in \mathcal{I}_n} T_{\mathsf{f}}(\mathsf{x}; \mathsf{p}^i)$, then $\mathfrak{V}^i = \mathfrak{I}^{-1}(i) = \{\mathbf{P}(\mathsf{x}, z) : (\mathsf{x}, z) \in \mathcal{S}_{\mathcal{P}} \cap \mathcal{S}_i\}$, and $\mathfrak{V} = \{\mathfrak{V}^i : i \in \mathcal{I}_n\}$. The situation is illustrated in Fig. 2(a) for the case when $n = 2$. In this figure, we observe that the common boundary of the cells $\mathfrak{V}^1$ and $\mathfrak{V}^2$ is the projection of the intersection of the cost surfaces $\mathcal{S}_1$ and $\mathcal{S}_2$ on the $x - y$ plane. Note that the points in $\mathfrak{R}(\mathcal{P})$ at which $\mathfrak{I}$ attains multiple values belong to the intersection of the common boundaries of neighboring cells of the partition $\mathfrak{V}$ generated by $\mathcal{P}$.

It follows readily from the previous discussion that for the characterization of the partition $\mathfrak{V} = \{\mathfrak{V}^i,\ i \in \mathcal{I}_n\}$, we need to carry out two basic tasks. First, we need to construct the surfaces $\mathcal{S}_i$, for each $i \in \mathcal{I}_n$, and second, determine their tightest (common) lower envelope $\mathcal{S}_{\mathcal{P}}$. The second task is a well-studied problem in computational geometry. We briefly mention two approaches one can adopt to compute the tightest lower envelope of a family of surfaces. The first approach is to apply techniques from algorithmic geometry [22] aimed at characterizing the tightest lower envelope of a finite set of functions [21] by forming the union of different curved facets. A detailed description of this approach for the one-dimensional case can be found in [22, pp. 355–358]. An alternative approach, is to use the so-called graphics hardware techniques [23,24]. It should be mentioned that when some of the parametric surfaces $\mathcal{S}_i$ are induced by discontinuous minimum time-to-go functions, it is important to have a priori knowledge of the structure and the key properties of the optimal synthesis of

the i–th NP, and in particular, the locations where the minimum time-to-go function undergoes discontinuous jumps.

Next, we focus on the characterization of each surface $\mathcal{S}_i$. Before we discuss the details of the computation of these cost surfaces, we introduce the τ-level set of the minimum time-to-go function $\ell_\tau(\mathsf{p}^i)$ emanating from $\mathsf{p}^i \in \mathcal{P}$, where $\ell_\tau(\mathsf{p}^i) := \{\mathsf{x} \in \mathfrak{R}(\mathsf{p}^i) : \ T_\mathsf{f}(\mathsf{x}; \mathsf{p}^i) = \tau\}$. Note that, in general, $\ell_\tau(\mathsf{p}^i)$ is a proper subset of $\mathfrak{R}_\tau(\mathsf{p}^i)$, that is, there exist points in $\mathfrak{R}_\tau(\mathsf{p}^i)$ that can also be reached at time less than τ. The following, less obvious, result highlights the relation between the level sets and the reachable sets of the i–th NP.

Proposition 2 *Let $0 \leq \tau < \infty$ and $\mathsf{p}^i \in \mathcal{P}$ be given. Under the assumptions of Proposition 1, $\mathfrak{R}_{t\leq\tau}(\mathsf{p}^i) = \bigcup_{0\leq t\leq\tau} \ell_t(\mathsf{p}^i)$.*

PROOF. Let $\mathsf{x} \in \mathfrak{R}_{t\leq\tau}(\mathsf{p}^i)$. Then in light of Proposition 1, $\mathsf{x} \in \ell_{T_\mathsf{f}(\mathsf{x};\mathsf{p}^i)}(\mathsf{p}^i)$, where $T_\mathsf{f}(\mathsf{x};\mathsf{p}^i) \leq \tau$, which implies, in turn, that $\mathsf{x} \in \bigcup_{0\leq t\leq\tau} \ell_t(\mathsf{p}^i)$. Conversely, let $\mathsf{x} \in \bigcup_{0\leq t\leq\tau} \ell_t(\mathsf{p}^i)$. The fact that $\ell_t(\mathsf{p}^i) \subseteq \mathfrak{R}_t(\mathsf{p}^i)$, for all $0 \leq t \leq \tau$, implies that $\mathsf{x} \in \bigcup_{0\leq t\leq\tau} \mathfrak{R}_t(\mathsf{p}^i) = \mathfrak{R}_{t\leq\tau}(\mathsf{p}^i)$. The result follows readily. ■

Corollary 1 *Given $\mathsf{p}^i \in \mathcal{P}$, it holds that $\mathfrak{R}(\mathsf{p}^i) = \bigcup_{0\leq t<\infty} \ell_t(\mathsf{p}^i)$.*

Proposition 2 and Corollary 1 imply a straightforward scheme to compute the cost surfaces $\mathcal{S}_i$ by propagating the minimum-time τ-level sets $\ell_\tau(\mathsf{p}^i)$, for $0 \leq \tau < \infty$. Before we describe this scheme, let us first define the lifted τ-level set $\Lambda_\tau(\mathsf{p}^i)$, which consists of the points $(\mathsf{x}, z) \in \mathfrak{R}(\mathsf{p}^i) \times [0, \infty)$, where $\mathsf{x} \in \ell_\tau(\mathsf{p}^i)$ and $z = T_\mathsf{f}(\mathsf{x}; \mathsf{p}^i)$. Note that an immediate consequence of Proposition 2 is that $\mathcal{S}_i = \bigcup_{0\leq\tau<\infty} \Lambda_\tau(\mathsf{p}^i)$.

Therefore, the computation of the cost surfaces $\mathcal{S}_i$ can be done as follows. First, compute the minimum-time level sets $\ell_\tau(\mathsf{p}^i)$, for $0 \leq \tau < \infty$. Subsequently, lift $\ell_t(\mathsf{p}^i)$ to the corresponding $\Lambda_t(\mathsf{p}^i)$, for all $0 \leq t < \infty$. Then the union of all the point-sets $\Lambda_\tau(\mathsf{p}^i)$, for $0 \leq \tau < \infty$, constitutes the cost surface $\mathcal{S}_i$. The situation is illustrated in Fig. 2(b).

Two techniques that address the problem of propagating the t-level sets for the special case of time-invariant drift fields and which are based, respectively, on a particle method and a fast marching method [37] are presented in [13,14]. Next, we present a more straightforward method to solve Problem 2 which, in contrast to the numerical techniques presented in [13,14], exploits the structure of the solution of the i–th NP.

3.2 Structure of Optimal Solutions for the i–th Navigation Problem

In order to pave the way for the characterization of the level sets of the minimum time-to-go function and subsequently the cost surface emanating from each generator, we first need to present some key results from the solution of the i–th NP, which, as already mentioned, is a special case of the ZNP. The reader interested in a detailed treatment of the ZNP based on standard tools from calculus of variations may refer to [25, pp. 239-247, pp. 370-373].

We adopt an approach based on optimal control theory, similar in spirit to the treatment of the ZNP presented in [26]. In particular, we define the Hamiltonian $\mathcal{H} : [0,\infty) \times \mathbb{R}^2 \times \mathbb{R}^2 \times U \mapsto \mathbb{R}$, by $\mathcal{H}(t, \mathsf{x}^i, \lambda^i, u^i) := \pi^i + \langle \lambda^i, w(t, \mathsf{x}^i) + u^i \rangle$, where $\lambda^i : [0,\infty] \mapsto \mathbb{R}^2$ and $\pi^i \leq 0$. In light of the Pontryagin Maximum Principle (PMP) [38], if $t \mapsto \mathsf{x}^i_*(t)$ is a minimum-time trajectory of the i–th NP generated by the minimum-time control $u^i_* \in \mathcal{U}$, then there exists a scalar $\pi^i_* \in \{-1, 0\}$ and an absolutely continuous function $t \mapsto \lambda^i_*(t)$ (the costate) such that

(i) $\lambda^i_*(t)$ and π^i_* cannot vanish simultaneously, that is, $|\lambda^i_*(t)| + |\pi^i_*| \neq 0$, for all $t \in [0, T_\mathsf{f}(\mathsf{x}; \mathsf{p}^i)]$.

(ii) $\lambda^i_*(t)$ satisfies the canonical equation

$$\dot{\lambda}^i_* = -\partial\mathcal{H}(t, \mathsf{x}^i_*, \lambda^i_*, u^i_*)/\partial\mathsf{x} = -\,\mathsf{A}_w{}^\mathsf{T}(t)\lambda^i_*, \quad (4)$$

where $\mathsf{A}_w(t) := \partial w(t, \mathsf{x}^i_*(t))/\partial\mathsf{x}$.

(iii) $\lambda^i_*(T_\mathsf{f})$ satisfies the transversality condition $\mathcal{H}(T_\mathsf{f}, \mathsf{x}^i_*(T_\mathsf{f}), \lambda^i_*(T_\mathsf{f}), u^i_*(T_\mathsf{f})) = 0$.

(iv) The optimal control u^i_* maximizes the Hamiltonian along the optimal state and costate trajectories, that is, $\mathcal{H}(t, \mathsf{x}^i_*, \lambda^i_*, u^i_*) \geq \mathcal{H}(t, \mathsf{x}^i_*, \lambda^i_*, v)$, for all $v \in U$.

Lemma 1 *The function $t \mapsto \lambda^i_*(t)$ does not vanish for all $t \in [0, T_\mathsf{f}(\mathsf{x}; \mathsf{p}^i)]$.*

PROOF. Assume, on the contrary, that there exists $\tau_0 \in [0, T_\mathsf{f}(\mathsf{x}; \mathsf{p}^i)]$ such that $\lambda^i_*(\tau_0) = 0$. Because λ^i_* satisfies the linear homogeneous differential equation (4), the condition $\lambda^i_*(\tau_0) = 0$ implies that $\lambda^i_*(t) = 0$ for all $t \in [0, T_\mathsf{f}(\mathsf{x}; \mathsf{p}^i)]$. Consequently, in light of PMP (condition (iii)), $\pi^i_* = 0$ and thus $|\lambda^i_*(t)| + |\pi^i_*| = 0$ for all $t \in [0, T_\mathsf{f}(\mathsf{x}; \mathsf{p}^i)]$, which contradicts condition (i) of PMP. This completes the proof. ■

An immediate consequence of PMP (condition (iv)) is that the optimal control is given by

$$u^i_*(t) = \lambda^i_*(t)/|\lambda^i_*(t)|, \quad (5)$$

where $|\lambda^i_*(t)| \neq 0$ in light of Lemma 1. In addition, it can be shown that the candidate minimum-time control law u^i_* of the i–th NP problem has necessarily the following structure: $u^i_*(t) = [\cos\theta^i_*(t), \ \sin\theta^i_*(t)]^\mathsf{T}$, where θ^i_* satisfies, for all $t \in [0, T_\mathsf{f}(\mathsf{x}; \mathsf{p}^i)]$, the following differential equation [25]

$$\begin{aligned}\dot{\theta}^i_* = {} & \mathrm{c}(t)\mathrm{s}(t)\left(\partial w_1(t, \mathsf{x}^i_*)/\partial x - \partial w_2(t, \mathsf{x}^i_*)/\partial y\right) \\ & + \mathrm{s}^2(t)\partial w_2(t, \mathsf{x}^i_*)/\partial x - \mathrm{c}^2(t)\partial w_1(t, \mathsf{x}^i_*)/\partial y, \quad (6)\end{aligned}$$

where $\mathrm{c}(t) := \sin\theta^i_*(t)$, $\mathrm{s}(t) := \cos\theta^i_*(t)$, $\theta^i_*(0) = \bar\theta^i \in [0, 2\pi)$, and w_1, w_2 denote, respectively, the x and y components of the drift field w. From (6) it follows that the (candidate) optimal control u^i_* is determined up to a single parameter, namely $\bar\theta^i$. We henceforth denote this fact by writing $u^i_*(\cdot;\bar\theta^i)$. Note that, as highlighted in [26], Eq. (6) can be viewed as a generalized Euler-Lagrange equation for the i–th NP, which is *not* equivalent to the stronger condition (iv) of PMP. In particular, the (candidate) optimal control $u^i_*(t) = [\cos\theta^i_*(t),\ \ \sin\theta^i_*(t)]^\mathsf{T}$, where θ^i_* satisfies (6), may correspond to the dual problem of the i–th NP, where one is interested in maximizing, rather than minimizing, the final time. In other words, Eq. (6) holds not only when u^i_* is the global maximum of the Hamiltonian along the optimal state and costate trajectories, by virtue of condition (iv) of PMP, but also when it is simply one of its extrema. For this reason, we henceforth refer to the candidate optimal control $u^i_*(\cdot;\bar\theta^i)$ as the *extremal control* of the i–th NP and the mapping $t \mapsto \mathsf{x}^i_*(t;\mathsf{p}^i,\bar\theta^i)$ as the *extremal trajectory* of the i–th NP generated by the extremal control $u^i_*(\cdot;\bar\theta^i)$. Finally, we refer to the admissible pair (x^i_*, u^i_*) as the extremal pair of the i–th NP.

Definition 1 *Let (x^i_*, u^i_*) be an extremal pair of the i–th NP. If $\pi^i_* = 0$, the mapping $t \mapsto \mathsf{x}^i_*(t;\mathsf{p}^i,u^i_*)$ is an abnormal extremal trajectory of the i–th NP. In addition, if $\pi^i_* = -1$ (resp., $\pi^i_* = 1$), the mapping $t \mapsto \mathsf{x}^i_*(t;\mathsf{p}^i,u^i_*)$ is a regular extremal trajectory of the minimum time i–th NP (resp., the maximum-time i–th NP).*

Next, we provide necessary and sufficient conditions for an extremal trajectory of the i–th minimum or maximum time NP to be either abnormal or regular.

Proposition 3 *Let (x^i_*, u^i_*) be an extremal pair of the i–th NP for a given terminal point x and let $E(t;\bar\theta^i) := \langle w(t,\mathsf{x}^i_*(t)), u^i_*(t;\bar\theta^i)\rangle + 1$. Then the mapping $t \mapsto \mathsf{x}^i_*(t;\mathsf{p}^i,u^i_*)$ is an abnormal extremal trajectory of the i–th NP if and only if $E(0;\bar\theta^i) = 0$.*

PROOF. For an abnormal extremal trajectory, $\pi^i_* = 0$. In addition, the transversality condition (condition (iii) of PMP) along with Eq. (5) and the fact that $|u^i_*(t;\bar\theta^i)| = 1$ for all $t \in [0, T_\mathsf{f}]$, where $T_\mathsf{f} = T_\mathsf{f}(\mathsf{x};\mathsf{p}^i)$, imply that

$$\begin{aligned} 0 &= \langle \lambda^i_*(T_\mathsf{f}), w(T_\mathsf{f},\mathsf{x}^i_*) + u^i_*(T_\mathsf{f};\bar\theta^i)\rangle \\ &= |\lambda^i_*(T_\mathsf{f})|(\langle u^i_*(T_\mathsf{f};\bar\theta^i), w(T_\mathsf{f},\mathsf{x}^i_*(T_\mathsf{f})\rangle + 1) \\ &= |\lambda^i_*(T_\mathsf{f})| E(T_\mathsf{f};\bar\theta^i). \end{aligned} \tag{7}$$

From Lemma 1, it follows that $\lambda^i_*(T_\mathsf{f}(\mathsf{x};\mathsf{p}^i)) \neq 0$, and thus (7) implies that $E(T_\mathsf{f}(\mathsf{x};\mathsf{p}^i);\bar\theta^i) = 0$. We claim that $E(T_\mathsf{f}(\mathsf{x};\mathsf{p}^i);\bar\theta^i) = 0$ implies, in turn, that $E(0;\bar\theta^i) = 0$. To see this, let us assume, on the contrary, that $E(0;\bar\theta^i) \neq 0$. Without loss of generality, assume that $E(0;\bar\theta^i) > 0$. Next, we make use of the result from the solution of the ZNP [25, pp 370–373] that, for all $t \in [0, T_\mathsf{f}(\mathsf{x};\mathsf{p}^i)]$, the sign of $E(t;\bar\theta^i)$ is the same as the sign of the function $\omega : [0,\infty) \mapsto \mathbb{R}$, which solves the linear homogeneous differential equation $\dot\omega(t) = \xi(t)\omega(t)$, where

$$\begin{aligned} \xi(t) = &-\mathrm{c}^2(t)\partial w_1(t,\mathsf{x}^i_*(t))/\partial x - \mathrm{s}^2(t)\partial w_2(t,\mathsf{x}^i_*(t))/\partial y \\ &- \mathrm{s}(t)\mathrm{c}(t)\left(\partial w_1(t,\mathsf{x}^i_*(t))/\partial y + \partial w_2(t,\mathsf{x}^i_*(t))/\partial x\right). \end{aligned}$$

Since $\omega(t) = \omega(0)\exp(\int_0^t \xi(\sigma)\mathrm{d}\sigma)$, it follows that $\omega(t)$ preserves the sign of $\omega(0)$, for all $t \in [0, T_\mathsf{f}(\mathsf{x};\mathsf{p}^i)]$. By hypothesis $E(0;\bar\theta^i) > 0$, and thus $\omega(0) > 0$. Therefore, $\omega(T_\mathsf{f}(\mathsf{x};\mathsf{p}^i)) > 0$, which implies, in turn, that $E(T_\mathsf{f}(\mathsf{x};\mathsf{p}^i);\bar\theta^i) > 0$, leading to a contradiction.

The converse can be proven similarly. ■

Corollary 2 *Let (x^i_*, u^i_*) be an extremal pair of the i–th NP. Then the mapping $t \mapsto \mathsf{x}^i_*(t;\mathsf{p}^i,u^i_*)$ is a regular extremal trajectory of the minimum (resp, maximum) time i–th NP if and only if $E(0;\bar\theta^i) > 0$ (resp., $E(0;\bar\theta^i) < 0$),*

An important observation from Proposition 3 and Corollary 2 is that the sign of E needs to be checked only at time $t = 0$. As shown next, an alternative way to distinguish between a regular extremal trajectory of the minimum or the maximum time i–th NP and an abnormal extremal trajectory of the i–th NP is by determining whether the angle between the forward and the inertial velocities of the i–th vehicle at time $t = 0$ is, respectively, an acute, obtuse or right angle.

Corollary 3 *Let (x^i_*, u^i_*) be an extremal pair of the i–th NP. Then the mapping $t \mapsto \mathsf{x}^i_*(t;\mathsf{p}^i,u^i_*)$ is a regular extremal trajectory of the minimum (resp., maximum) time i–th NP if and only if $\langle \dot{\mathsf{x}}^i_*(0), u^i_*(0;\bar\theta^i)\rangle > 0$ (resp., $\langle \dot{\mathsf{x}}^i_*(0), u^i_*(0;\bar\theta^i)\rangle < 0$). Furthermore, the mapping $t \mapsto \mathsf{x}^i_*(\cdot;\mathsf{p}^i,u^i_*)$ is an abnormal extremal trajectory of either the minimum or the maximum time i–th NP if and only if $\langle \dot{\mathsf{x}}^i_*(0), u^i_*(0;\bar\theta^i)\rangle = 0$.*

PROOF. For $t \geq 0$, we have that $\langle \dot{\mathsf{x}}^i_*(t), u^i_*(t;\bar\theta^i)\rangle = \langle w(t,\mathsf{x}^i_*(t)), u^i_*(t;\bar\theta^i)\rangle + 1$. Therefore, $\langle \dot{\mathsf{x}}^i_*(t), u^i_*(t;\bar\theta^i)\rangle = E(t;\bar\theta^i)$, for all $t \in [0, T^i_\mathsf{f}]$. The result follows readily from Proposition 3 and Corollary 2. ■

Remark 2 The reader should not hastily jump to the erroneous conclusion that a regular extremal trajectory $t \mapsto \mathsf{x}^i_*(t;\mathsf{p}^i,\bar\theta^i)$ for which $E(0;\bar\theta^i) < 0$ is a minimum time trajectory of the i–th NP, for all $t \geq 0$. This is not true, in general, as we will see in the subsequent analysis.

The next proposition provides conditions for the existence as well as the number of abnormal extremal trajectories of the i–th NP, which can emanate from some $\mathsf{p}^i \in \mathcal{P}$.

Proposition 4 *Let $(t,\mathsf{x}^i) \mapsto w(t,\mathsf{x}^i)$ be a (time-varying) drift field that satisfy the condition (2). If $|w(0,\mathsf{p}^i)| > 1$, then the i–th NP admits exactly two abnormal extremal trajectories emanating from p^i. If $|w(0,\mathsf{p}^i)| < 1$, then the i–th NP admits only regular extremal trajectories emanating from p^i. If $|w(0,\mathsf{p}^i)| = 1$,*

then the i–th NP admits a unique abnormal extremal trajectory emanating from p^i.

PROOF. It follows from Corollary 3 that the values of $\bar{\theta}^i$ corresponding to abnormal extremal trajectories of the i–th NP are necessarily solutions of the following equation $\langle w(0,\mathsf{p}^i),\mathrm{e}_1\rangle\cos\bar{\theta}^i + \langle w(0,\mathsf{p}^i),\mathrm{e}_2\rangle\sin\bar{\theta}^i = -1$, where $\mathrm{e}_1 = [1,\ 0]^\mathsf{T}$ and $\mathrm{e}_2 = [0,\ 1]^\mathsf{T}$, or equivalently, $|w(0,\mathsf{p}^i)|\cos(\bar{\theta}^i - \varphi_w(0,\mathsf{p}^i)) = -1$, where $\varphi_w(0,\mathsf{p}^i) := \operatorname{atan}_2(\langle w(0,\mathsf{p}^i),\mathrm{e}_2\rangle,\langle w(0,\mathsf{p}^i),\mathrm{e}_1\rangle)$. If $|w(0,\mathsf{p}^i)| > 1$ (resp. $|w(0,\mathsf{p}^i)| < 1$), then the last equation has exactly two solutions in $[0,2\pi)$ (resp. has no solution at all), whereas it admits a unique solution in $[0,2\pi)$, when $|w(0,\mathsf{p}^i| = 1$. ■

Figure 3 illustrates the extremal trajectories of the system (1), also known as the *field of extremals* [27,25,39], emanating from some $\mathsf{p}^i \in \mathcal{P}$, driven by the candidate optimal control $u^i_*(\cdot;\bar{\theta}^i)$ after all maximizing trajectories have been removed. The following qualitative discussion, which extends the discussion presented in [25] and [26,40], will shed light on some important features of the optimal synthesis of the ZNP. In particular, we describe the qualitative behavior of the minimum time-to-go function, in the case of a spatially and time-varying drift field that satisfies (2), in relation with the presence or absence of abnormal extremal trajectories of the i–th NP. In particular, there are three cases of interest based on the relative position of p^i with respect to the set $\Omega := \{\mathsf{x}\in\mathbb{R}^2 :\ |w(0,\mathsf{x})| < 1\}$.

In the first case, we assume that p^i belongs to the complement of the closure of Ω. In this case $|w(0,\mathsf{x}^i)| > 1$, which implies that the local drift exceeds the magnitude of the forward velocity of the i–th vehicle. Consequently, the i–th vehicle cannot move to every possible direction. In particular, if $|w(t,\mathsf{x}^i)| > 1$, then, at time t, the vehicle's inertial velocity $\dot{\mathsf{x}}^i := w(t,\mathsf{x}^i) + u^i$, is constrained to lie, for all $u^i \in \mathcal{U}$, within a cone $\mathcal{K}(t,\mathsf{x}^i)$ of allowable directions. As shown in [41], $\mathcal{K}(t,\mathsf{x}^i)$ is a right (non-oblique) cone of angle $\vartheta_\mathcal{K}(t,\mathsf{x}^i) := 2\arcsin(1/|w(t,\mathsf{x}^i)|)$, whose apex is x^i (current position of the i–th vehicle) and its axis is parallel to $w(t,\mathsf{x}^i)$. Consequently, p^i may either remain on the boundary of its reachable set for all $t \geq 0$ or there may exist a time $t = \tau_1 > 0$ such that p^i lies on the boundary of $\mathfrak{R}_{t\leq\tau}(\mathsf{p}^i)$, for all $0 < \tau \leq \tau_1$, and on the interior of $\mathfrak{R}_{t\leq\tau}(\mathsf{p}^i)$, for $\tau > \tau_1$. The situation is illustrated in Fig. 3(b), where we observe the existence of extremal trajectories $t \mapsto \mathsf{x}^i_*(t;\mathsf{p}^i,\bar{\theta}^i)$ that are (globally) minimum-time trajectories of the i–th NP until some finite time at which they visit points that have already been visited by different extremal trajectories emanating from p^i (trajectories that correspond to different values of $\bar{\theta}^i$).

As we have already shown in Proposition 4, when $|w(0,\mathsf{x}^i)| > 1$, there exist two abnormal trajectories emanating from p^i, which are denoted by $\tilde{\mathsf{x}}^i_1$ and $\tilde{\mathsf{x}}^i_2$ in Fig. 3(b). As shown in Fig. 3(b), regular extremals lose their optimality when they intersect with the manifolds determined by the abnormal extremal trajectories $\tilde{\mathsf{x}}^i_1$ and (part of) $\tilde{\mathsf{x}}^i_2$ for the first time. The suboptimal parts of the extremal trajectories after the latter have crossed the manifolds determined by the abnormal extremal trajectories $\tilde{\mathsf{x}}^i_1$ and (part of) $\tilde{\mathsf{x}}^i_2$ correspond to the magenta curve segments in Fig. 3(b). Note that, for the particular example illustrated in Fig. 3(b), the i-th vehicle can reach every point in the plane although initially it was unable to move to every possible direction as a consequence of the fact that $|w(0,\mathsf{x}^i)| > 1$. Another important observation is that the minimum time-to-go function undergoes discontinuous jumps, which occur at points that belong to the manifolds determined by the two abnormal extremal trajectories of the i–th NP.

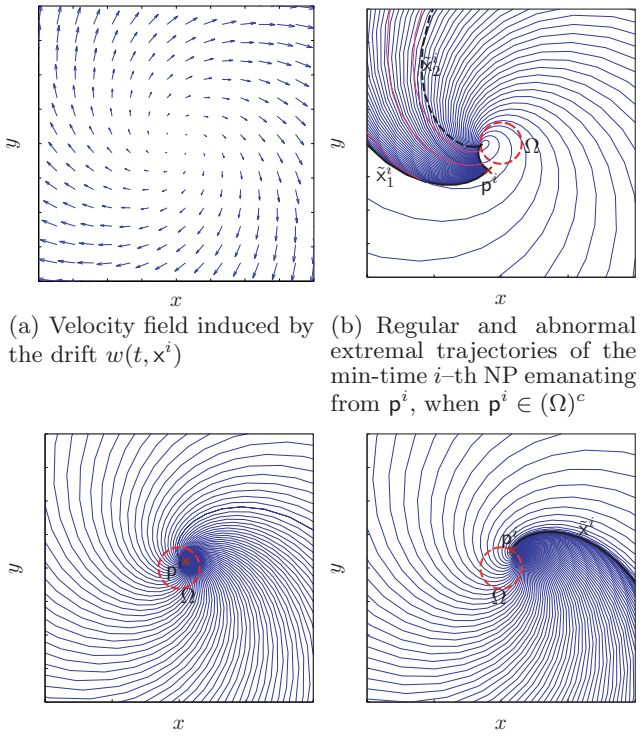

(a) Velocity field induced by the drift $w(t,\mathsf{x}^i)$

(b) Regular and abnormal extremal trajectories of the min-time i–th NP emanating from p^i, when $\mathsf{p}^i \in (\Omega)^c$

(c) Regular extremal trajectories of the min-time i–th NP emanating from p^i, when $\mathsf{p}^i \in \Omega$

(d) Regular and abnormal extremal trajectories of the min-time i–th NP emanating from p^i, when $\mathsf{p}^i \in \operatorname{bd}\Omega$

Fig. 3. Integral trajectories forming the flow of the system (1), also known as the "field of extremals", generated by the candidate optimal control $u_*(t;\bar{\theta}^i)$, for $t \geq 0$. Note that in (b) regular extremal trajectories lose their optimality as they intersect the abnormal extremal trajectories $\tilde{\mathsf{x}}^i_1$ and $\tilde{\mathsf{x}}^i_2$.

The second case we consider is when $\mathsf{p}^i \in \Omega$, that is, $|w(0,\mathsf{p}^i)| < 1$. In this case the i–th vehicle can move, at time $t = 0$, to every direction (for more details, see [41]). Consequently, $\mathsf{p}^i \in \operatorname{int}\mathfrak{R}_{t\leq\tau}(\mathsf{p}^i)$, for all $\tau \geq 0$. The third case we consider is when $\mathsf{p}^i \in \operatorname{bd}\Omega$, equivalently, when $|w(0,\mathsf{p}^i)| = 1$. In this case, there is a unique abnormal extremal trajectory, as shown in Proposition 4. An important observation is that the function $\mathsf{x} \mapsto T_\mathsf{f}(\mathsf{x};\mathsf{p}^i)$ undergoes discontinuous jumps at points that belong to the manifold determined by this abnormal extremal tra-

jectory.

3.3 *Characterization of the Level Sets of the Minimum Time-to-Go Function of the i–th NP*

Next, we proceed with the characterization of the level sets of the i–th NP by making use of the properties enjoyed by the solution of the ZNP.

Proposition 5 *Given $0 \leq \tau < \infty$ and $\mathsf{p}^i \in \mathcal{P}$, then $\ell_\tau(\mathsf{p}^i) \subseteq \mathrm{bd}\mathfrak{R}_\tau(\mathsf{p}^i)$.*

PROOF. The proof follows readily, by making use of Corollary 1 in [34, pp.75–76]. ■

In light of Proposition 5, the set $\mathrm{bd}\mathfrak{R}_\tau(\mathsf{p}^i)$, whose computation may not be a simple task, provides a conservative estimate of the level set $\ell_\tau(\mathsf{p}^i)$. This conservatism is owing to the fact that $\mathrm{bd}\mathfrak{R}_\tau(\mathsf{p}^i)$ may consist of endpoints of trajectories that do not satisfy the necessary conditions for optimality given in Section 3.2. Next, we introduce an alternative estimate of $\ell_\tau(\mathsf{p}^i)$, which exploits Propositions 3 and Corollary 2. In particular, we consider, for a given $\tau > 0$, the set $\mathfrak{K}^*_\tau(\mathsf{p}^i) := \bigcup_{\bar\theta^i \in [0,2\pi)} \{\mathsf{x} = \mathsf{x}^i_*(\tau; \mathsf{p}^i, \bar\theta^i) : \ E(0; \bar\theta^i) \geq 0\}$. Note that $\mathfrak{K}^*_\tau(\mathsf{p}^i)$ consists of the endpoints of all extremal trajectories of the i–th NP, except from the endpoints of regular extremal trajectories of the maximum time i–th NP.

Proposition 6 *Given $0 \leq \tau < \infty$ and $\mathsf{p}^i \in \mathcal{P}$, then $\ell_\tau(\mathsf{p}^i) \subseteq \mathfrak{K}^*_\tau(\mathsf{p}^i)$.*

Proposition 6 implies that the set $\mathfrak{K}^*_\tau(\mathsf{p}^i)$ provides a conservative estimate of the level set $\ell_\tau(\mathsf{p}^i)$, for a given $\tau > 0$. This conservatism is owing to the fact that regular extremal trajectories of the minimum-time i–th NP may lose optimality after some finite time. In particular, regular extremal trajectories may visit at some time $t = \tau_1 < \tau$ points that belong to the reachable set $\mathfrak{R}_{\tau_0}(\mathsf{p}^i)$, where $\tau_0 < \tau_1 < \tau$, as we have already mentioned in Section 3.2. More precisely, for a given $0 < \tau < \infty$, there may exist $0 < \tau_0 < \tau$ such that $\mathfrak{R}_{t \leq \tau_0}(\mathsf{p}^i) \cap \mathfrak{K}^*_\tau(\mathsf{p}^i) \neq \varnothing$. If $\mathsf{x} \in \mathfrak{R}_{t \leq \tau_0}(\mathsf{p}^i) \cap \mathfrak{K}^*_\tau(\mathsf{p}^i)$, for $\tau_0 < \tau$, then $\mathsf{x} \notin \ell_\tau(\mathsf{p}^i)$, since $T_\mathsf{f}(\mathsf{x}; \mathsf{p}^i) \leq \tau_0 < \tau$. Therefore, in order to further refine this estimate of the level set $\ell_\tau(\mathsf{p}^i)$, we need to remove from $\mathfrak{K}^*_\tau(\mathsf{p}^i)$ all these points that can be reached faster than τ units of time.

Proposition 7 *Let $\tau > 0$ and $\mathsf{p}^i \in \mathcal{P}$ be given. Then $\mathsf{x} \in \ell_\tau(\mathsf{p}^i)$ if and only if $\mathsf{x} \in \mathfrak{K}^*_\tau(\mathsf{p}^i)$ and $\mathsf{x} \notin \mathfrak{R}_{\tau_0}(\mathsf{p}^i)$, for all $0 \leq \tau_0 < \tau$.*

PROOF. Let $\mathsf{x} \in \ell_\tau(\mathsf{p}^i)$. In light of Proposition 6, it follows that $\mathsf{x} \in \mathfrak{K}^*_\tau(\mathsf{p}^i)$. Let us assume, on the contrary, that there exists $0 \leq \tau_0 < \tau$ such that $\mathsf{x} \in \mathfrak{R}_{\tau_0}(\mathsf{p}^i)$. Because $\mathsf{x} \in \ell_\tau(\mathsf{p}^i)$, it follows that $\tau = T_\mathsf{f}(\mathsf{x}; \mathsf{p}^i)$. However, the point x can be reached from p^i at time $t = \tau_0 < \tau = T_\mathsf{f}(\mathsf{x}; \mathsf{p}^i)$, leading to a contradiction.

Conversely, let $\mathsf{x} \in \mathfrak{K}^*_\tau(\mathsf{p}^i)$ and $\mathsf{x} \notin \mathfrak{R}_{\tau_0}(\mathsf{p}^i)$, for all $0 \leq \tau_0 < \tau$. In light of Proposition 1, there exists $\tau_\star \geq 0$ such that $\mathsf{x} \in \ell_{\tau_\star}(\mathsf{p}^i) \neq \varnothing$. Since $\mathsf{x} \notin \mathfrak{R}_{\tau_0}(\mathsf{p}^i)$, for all $0 \leq \tau_0 < \tau$, it follows that $\tau_\star \geq \tau$. Now let us assume, on the contrary, that $\tau_\star > \tau$. Consequently, x cannot be reached at $t = \tau$, which contradicts the fact that $\mathsf{x} \in \mathfrak{K}^*_\tau(\mathsf{p}^i) \subseteq \mathfrak{R}_\tau(\mathsf{p}^i)$. Therefore, $\tau_\star = \tau$, and thus $\mathsf{x} \in \ell_\tau(\mathsf{p}^i)$. This completes the proof. ■

Figure 4 illustrates the sets $\mathfrak{K}^*_\tau(\mathsf{p}^i)$ and $\ell_\tau(\mathsf{p}^i)$ for different values of $\tau \in [0, \infty)$ and two different drift fields (see also Fig. 1). For the first drift field, the computation of the set $\mathfrak{K}^*_\tau(\mathsf{p}^i)$ suffices to characterize the level set $\ell_\tau(\mathsf{p}^i)$, as is illustrated in Fig. 4(a). The situation is different for the second drift field, where the sets $\mathfrak{K}^*_\tau(\mathsf{p}^i)$, for different $\tau > 0$, may be supersets of their corresponding level sets $\ell_\tau(\mathsf{p}^i)$. The situation is illustrated in Fig. 4(b), where the red dashed parts of the $\mathfrak{K}^*_\tau(\mathsf{p}^i)$ correspond to the set $\mathfrak{K}^*_\tau(\mathsf{p}^i) \backslash \ell_\tau(\mathsf{p}^i)$, that is, the set that consists of the points that can be reached faster than τ units of time (these points belong to the suboptimal parts of regular extremal trajectories that lose their optimality after some finite time, as we have discussed previously).

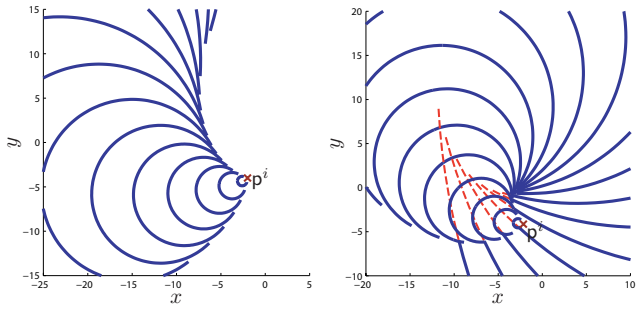

(a) $\ell_\tau(\mathsf{p}^i) = \mathfrak{K}^*_\tau(\mathsf{p}^i)$. (b) $\ell_\tau(\mathsf{p}^i) \subseteq \mathfrak{K}^*_\tau(\mathsf{p}^i)$.

Fig. 4. The level set $\ell_\tau(\mathsf{p}^i)$ is, in general, a subset of the set $\mathfrak{K}^*_\tau(\mathsf{p}^i)$. While the two sets are identical in Fig. 4(a), this is not the case in Fig. 4(b), where the red dashed lines correspond to the "excessive" part of $\mathfrak{K}^*_\tau(\mathsf{p}^i)$, that is, the set $\mathfrak{K}^*_\tau(\mathsf{p}^i) \backslash \ell_\tau(\mathsf{p}^i)$.

4 Topological Properties of the ZVD

In this section, we establish some topological properties enjoyed by the generators and the cells of the ZVD. First, we examine under what conditions a generator of the ZVD is an interior or a boundary point of its associated cell.

Proposition 8 *Let $\mathfrak{V} := \{\mathfrak{V}^i, \ i \in \mathcal{I}_n\}$ be the ZVD generated by the set $\mathcal{P}$. If $\mathsf{p}^i \in \operatorname{int} \mathfrak{R}_{t \leq \tau}(\mathsf{p}^i)$ for all $\tau > 0$, then $\mathsf{p}^i \in \operatorname{int} \mathfrak{V}^i$.*

PROOF. Let $\tau > 0$. By hypothesis, there exists $\varepsilon_1 = \varepsilon_1(\tau) > 0$, such that $B_{\varepsilon_1}(\mathsf{p}^i) := \{\mathsf{x} : |\mathsf{x} - \mathsf{p}^i| < \varepsilon_1\} \subseteq \mathfrak{R}_{t \leq \tau}(\mathsf{p}^i)$. Let $j \neq i$. Because $\mathcal{P}$ consists of n distinct points, there exists a sufficiently small $\varepsilon_2 > 0$ such that $\mathsf{p}^j \notin B_{\varepsilon_2}(\mathsf{p}^i)$. Take $\varepsilon = \min\{\varepsilon_1, \varepsilon_2\}$. Next, we show that there always exists $\hat\tau^j > 0$ such that $\mathsf{p}^i \notin \mathfrak{R}_{t \leq \hat\tau^j}(\mathsf{p}^j)$.

We consider two cases. The first case is when $B_\varepsilon(\mathsf{p}^i) \cap \mathfrak{R}_{t \leq \tau}(\mathsf{p}^j) = \varnothing$. In this case we can simply take $\hat\tau^j = \tau$.

The second case is when $B_\varepsilon(\mathsf{p}^i) \cap \mathfrak{R}_{t\leq\tau}(\mathsf{p}^j) \neq \varnothing$. Denote by $\bar{\tau}$ the infimum over the set of times $t \leq \tau$ required for the system (1), starting from p^j at time $t = 0$, to reach the ball $B_\varepsilon(\mathsf{p}^i)$ for the first time. Take $\hat{\tau}^j = \min\{\tau, \bar{\tau}/2\}$. Then $B_\varepsilon(\mathsf{p}^i) \cap \mathfrak{R}_{t\leq\hat{\tau}^j}(\mathsf{p}^j) = \varnothing$.

Thus in both cases, $B_\varepsilon(\mathsf{p}^i) \cap \mathfrak{R}_{t\leq\hat{\tau}^j}(\mathsf{p}^j) = \varnothing$ and $B_\varepsilon(\mathsf{p}^i) \subseteq \mathfrak{R}_{t\leq\hat{\tau}^j}(\mathsf{p}^i)$. By taking $\hat{\tau} = \min_{j\neq i}\{\hat{\tau}^j\}$, it follows that there is no point in $\mathcal{P}\backslash\{\mathsf{p}^i\}$ from which the system (1) can reach $B_\varepsilon(\mathsf{p}^i)$ at time $t = \hat{\tau}$ or faster. Thus, by definition, $B_\varepsilon(\mathsf{p}^i) \subseteq \mathfrak{V}^i$, which implies, in turn, that $B_\varepsilon(\mathsf{p}^i) \subseteq \mathrm{int}\mathfrak{V}^i$ since $B_\varepsilon(\mathsf{p}^i)$ is open. Therefore, $\mathsf{p}^i \in \mathrm{int}\mathfrak{V}^i$, and this completes the proof. ■

Proposition 9 *Let $\mathfrak{V} := \{\mathfrak{V}^i,\ i \in \mathcal{I}_n\}$ be the ZVD generated by the set $\mathcal{P}$. If $\mathfrak{R}(\mathsf{p}^i) \subset \mathbb{R}^2$ and $\mathsf{p}^i \in \mathrm{bd}\mathfrak{R}(\mathsf{p}^i)$, then $\mathsf{p}^i \in \mathrm{bd}\mathfrak{V}^i$.*

PROOF. Assume, on the contrary, that $\mathsf{p}^i \in \mathrm{int}\mathfrak{V}^i$. Since by definition $\mathfrak{V}^i \subseteq \mathfrak{R}(\mathsf{p}^i)$, it follows readily that $\mathrm{int}\mathfrak{V}^i \subseteq \mathrm{int}\mathfrak{R}(\mathsf{p}^i)$. Thus, $\mathsf{p}^i \in \mathrm{int}\,\mathfrak{R}(\mathsf{p}^i)$, leading to a contradiction. ■

Remark 3 It is possible that, for some drift fields, there may exist τ_0 and $\tau > \tau_0$ such that $\mathsf{p}^i \in \mathrm{bd}\mathfrak{R}_{t\leq\tau_0}(\mathsf{p}^i)$ but $\mathsf{p}^i \in \mathrm{int}\mathfrak{R}_{t\leq\tau}(\mathsf{p}^i)$. In other words, there is a possibility that $\mathsf{p}^i \in \mathrm{int}\,\mathfrak{R}(\mathsf{p}^i)$ but $\mathsf{p}^i \notin \mathrm{int}\,\mathfrak{R}_{t\leq\tau}(\mathsf{p}^i)$ for all $\tau > 0$. Consequently, neither Proposition 8 nor Proposition 9 applies. This scenario is illustrated in Figs. 3(b) and 4(b). In this case, a generator $\mathsf{p}^i \in \mathcal{P}$ of the ZVD can either be an interior or a boundary point of its associated cell.

Another important question we wish to examine is under what conditions a cell of the ZVD is a connected set. In the case of a time invariant drift field, the authors of [13] present a brief discussion about the connectedness of each cell of the ZVD based on qualitative arguments. Next, we prove the connectedness of each cell of the ZVD in the case of a time-invariant drift field that satisfies (2).

Proposition 10 *Let $\mathfrak{V} := \{\mathfrak{V}^i,\ i \in \mathcal{I}_n\}$ be the ZVD generated by the set $\mathcal{P}$. If the drift field $(t, \mathsf{x}^i) \mapsto w(t, \mathsf{x}^i)$ is time-invariant, that is, for every $\mathsf{x}^i \in \mathbb{R}^2$, $w(\tau_0, \mathsf{x}^i) = w(\tau_1, \mathsf{x}^i)$, for all $\tau_0, \tau_1 \geq 0$, and satisfies the condition (2), then the cell $\mathfrak{V}^i$ is connected, for all $i \in \mathcal{I}_n$.*

PROOF. Let $\mathsf{x} \in \mathfrak{V}^i$ and let $t \mapsto \mathsf{x}^i_*(t; \mathsf{p}^i, \bar{\theta}^i)$ be the corresponding minimum-time trajectory of the i–th NP such that $\mathsf{x} = \mathsf{x}^i_*(T_\mathsf{f}(\mathsf{x}; \mathsf{p}^i); \mathsf{p}^i, \bar{\theta}^i)$. We wish to show that the point-set $\mathcal{D}_\mathsf{x}(\mathsf{p}^i) := \{\mathsf{x}^i_*(t; \mathsf{p}^i, \bar{\theta}^i) : t \in [0, T_\mathsf{f}(\mathsf{x}; \mathsf{p}^i)]\} \subseteq \mathfrak{V}^i$.

Let $\mathsf{y} \in \mathcal{D}_\mathsf{x}(\mathsf{p}^i)$ and let us assume, on the contrary, that there exists $j \neq i$ such that $\mathsf{y} \in \mathfrak{V}^j\backslash\mathfrak{V}^i$, which implies, in turn, that $T_\mathsf{f}(\mathsf{y}; \mathsf{p}^j) < T_\mathsf{f}(\mathsf{y}; \mathsf{p}^i)$. Now let $T_\mathsf{f}(\mathsf{x}; \mathsf{y}, \tau_0)$ denote the minimum time required to drive the system (1), starting from y at time $t = \tau_0$, to x. Because by assumption the drift field is time-invariant it holds that $T_\mathsf{f}(\mathsf{x}; \mathsf{y}, \tau_0) = T_\mathsf{f}(\mathsf{x}; \mathsf{y}, \tau_1)$, for all τ_0, $\tau_1 \geq 0$. By taking $\tau_0 = T_\mathsf{f}(\mathsf{y}; \mathsf{p}^i)$ and $\tau_1 = T_\mathsf{f}(\mathsf{y}; \mathsf{p}^j)$, it follows that $T_\mathsf{f}(\mathsf{x}; \mathsf{p}^i) = T_\mathsf{f}(\mathsf{y}; \mathsf{p}^i) + T_\mathsf{f}(\mathsf{x}; \mathsf{y}, T_\mathsf{f}(\mathsf{y}; \mathsf{p}^i)) = T_\mathsf{f}(\mathsf{y}; \mathsf{p}^i) + T_\mathsf{f}(\mathsf{x}; \mathsf{y}, T_\mathsf{f}(\mathsf{y}; \mathsf{p}^j))$. Now, if $T_\mathsf{f}(\mathsf{y}; \mathsf{p}^j) < T_\mathsf{f}(\mathsf{y}; \mathsf{p}^i)$, then

$$T_\mathsf{f}(\mathsf{x}; \mathsf{p}^i) > T_\mathsf{f}(\mathsf{y}; \mathsf{p}^j) + T_\mathsf{f}(\mathsf{x}; \mathsf{y}, T_\mathsf{f}(\mathsf{y}; \mathsf{p}^j)) = T_\mathsf{f}(\mathsf{x}; \mathsf{p}^j).$$

Therefore, we have shown that $T_\mathsf{f}(\mathsf{x}; \mathsf{p}^j) < T_\mathsf{f}(\mathsf{x}; \mathsf{p}^i)$, which contradicts the initial assumption that $\mathsf{x} \in \mathfrak{V}^i$. Hence, for every $\mathsf{x} \in \mathfrak{V}^i$, the set $\mathcal{D}_\mathsf{x}(\mathsf{p}^i) \subseteq \mathfrak{V}^i$. It follows that $\mathfrak{V}^i$ is path connected and hence connected. ■

In the case of a time-varying drift field, the connectedness of each cell of the ZVD is, in general, not guaranteed. The following proposition gives a sufficient condition for the connectedness of each cell of the ZVD for the case of a time-varying drift field that satisfies (2).

Proposition 11 *Let $(t, \mathsf{x}^i) \mapsto w(t, \mathsf{x}^i)$ be a (time-varying) drift field that satisfies the condition (2), and let $\mathfrak{V} := \{\mathfrak{V}^i,\ i \in \mathcal{I}_n\}$ be the ZVD generated by the set $\mathcal{P}$. Let us assume that, for all $i \in \mathcal{I}_n$, $\mathfrak{R}_{\tau_0}(\mathsf{p}^i) \subseteq \mathfrak{R}_{\tau_1}(\mathsf{p}^i)$, where $0 < \tau_0 \leq \tau_1 < \infty$, and $\mathsf{p}^i \in \mathrm{int}\,\mathfrak{R}_\tau(\mathsf{p}^i)$, for all $\tau > 0$. Then $\mathfrak{V}^i$ is connected, for all $i \in \mathcal{I}_n$.*

PROOF. It suffices to show that $\mathrm{int}\,\mathfrak{V}^i$ is connected. To this end, first notice that the conditions of Proposition 8 are satisfied and thus $\mathsf{p}^i \in \mathrm{int}\,\mathfrak{V}^i$, for all $i \in \mathcal{I}_n$. We claim that if $\mathsf{x} \in \mathrm{int}\,\mathfrak{V}^i$, then $\mathcal{D}_\mathsf{x}(\mathsf{p}^i) \subset \mathrm{int}\,\mathfrak{V}^i$. Let $\mathsf{y} \in \mathcal{D}_\mathsf{x}(\mathsf{p}^i)$ and let us assume, on the contrary, that there exists $j \neq i$ such that $\mathsf{y} \in \mathfrak{V}^j\backslash\mathfrak{V}^i$, which implies, in turn, that $T_\mathsf{f}(\mathsf{y}; \mathsf{p}^j) < T_\mathsf{f}(\mathsf{y}; \mathsf{p}^i)$. By hypothesis, and since $\mathsf{y} \in \mathfrak{R}_{T_\mathsf{f}(\mathsf{y};\mathsf{p}^j)}(\mathsf{p}^j)$, it follows that $\mathsf{y} \in \mathfrak{R}_{T_\mathsf{f}(\mathsf{y};\mathsf{p}^i)}(\mathsf{p}^j)$. Thus the system (1), starting from p^j at time $t = 0$, can reach y at time $t = T_\mathsf{f}(\mathsf{y}; \mathsf{p}^i)$ and subsequently reach x at time $t = T_\mathsf{f}(\mathsf{y}; \mathsf{p}^i) + T_\mathsf{f}(\mathsf{x}; \mathsf{y}, T_\mathsf{f}(\mathsf{y}; \mathsf{p}^i)) = T_\mathsf{f}(\mathsf{x}; \mathsf{p}^i)$. Let $\mathcal{T}_\mathsf{x}(\mathsf{p}^j) := \{\tau \geq 0 :\ \mathsf{x} \in \mathfrak{R}_\tau(\mathsf{p}^j)\}$. Note that the set $\mathcal{T}_\mathsf{x}(\mathsf{p}^j)$ consists of all the times τ such that the system (1), starting from p^j at time $t = 0$, can reach x at time $t = \tau$ with the application of an admissible control input. We have shown that $T_\mathsf{f}(\mathsf{x}; \mathsf{p}^i) \in \mathcal{T}_\mathsf{x}(\mathsf{p}^j)$. Because, by definition, $T_\mathsf{f}(\mathsf{x}; \mathsf{p}^j) = \inf \mathcal{T}_\mathsf{x}(\mathsf{p}^j)$, it follows readily that $T_\mathsf{f}(\mathsf{x}; \mathsf{p}^j) \leq T_\mathsf{f}(\mathsf{x}; \mathsf{p}^i)$, which contradicts the initial assumption that $\mathsf{x} \in \mathrm{int}\,\mathfrak{V}^i$. Therefore $\mathrm{int}\,\mathfrak{V}^i$ is path connected, and hence connected, which implies, in turn, that $\mathfrak{V}^i$ is also connected (Theorem 26.8 in [42]). ■

Note that if each cell of the ZVD is connected, then, as is shown in [14], the complexity of the data structure associated with the ZVD is linear to the number n of its generators. For example, the partition is completely characterized by n non-overlapping connected sets which are thus neighboring to at most $\mathcal{O}(n)$ cells from the same partition. The previous remark reflects the fact that, under the assumptions of Propositions 10-11, the computation and storage requirements of the ZVD are guaranteed to scale well with the problem data.

5 Simulation Results

In this section, we present numerical simulation results to illustrate the previous analysis. We consider a drift field of the form (3) with $\mathsf{A}(t) = \left[\begin{smallmatrix} \alpha(t) & \beta(t) \\ -\beta(t) & \alpha(t) \end{smallmatrix}\right]$ and $\nu(t) \equiv 0$. In this case, the candidate optimal control can be computed analytically. In particular, $u_*^i(t) = [\cos\theta_*^i(t), \quad \sin\theta_*^i(t)]^\mathsf{T}$, where $\theta_*^i = \bar{\theta}^i - \int_0^t \beta(\sigma)\,\mathrm{d}\sigma$. In addition, since $\mathsf{A}(t) = \alpha(t)\,\mathsf{I}_2 + \beta(t)\,\mathsf{J}_2$, where $\mathsf{I}_2 := \left[\begin{smallmatrix} 1 & 0 \\ 0 & 1 \end{smallmatrix}\right]$ and $\mathsf{J}_2 := \left[\begin{smallmatrix} 0 & 1 \\ -1 & 0 \end{smallmatrix}\right]$, it can be shown that the state transition matrix of $\mathsf{A}(t)$ is given by $\Phi(t,0) = \exp\left(\int_0^t \alpha(\sigma)\mathrm{d}\sigma\right) \left[\begin{smallmatrix} \cos\int_0^t \beta(\sigma)\mathrm{d}\sigma & \sin\int_0^t \beta(\sigma)\mathrm{d}\sigma \\ -\sin\int_0^t \beta(\sigma)\mathrm{d}\sigma & \cos\int_0^t \beta(\sigma)\mathrm{d}\sigma \end{smallmatrix}\right]$. From the state transition matrix $\Phi(t,0)$, we can directly compute first the reachable sets $\mathfrak{R}_\tau(\mathsf{p}^i)$ and the sign of the quantity $E(0;\bar{\theta}^i)$, and subsequently, the sets $\mathfrak{K}_\tau^*(\mathsf{p}^i)$, for all $\tau \geq 0$.

Figure 5 illustrates the ZVD generated by a point-set of nine generators for $\alpha = 0$, $\beta = 0.4t$ (time-varying field scenario) and $\alpha = 0.2$, $\beta = 0.2$ (time-invariant field scenario). In addition, Fig. 6 illustrates the level sets of the minimum time-to-go emanating from each generator restricted to their corresponding cell.

In Fig. 5, we observe that the cells and the generators of the ZVD do not enjoy the same topological properties with those of the standard Voronoi diagram generated by the same set of generators. In particular, the generators of the ZVD are not always interior points of their associated cells and the latter are non-convex sets. In addition, the neighboring relations between the generators of the ZVD are different than those of the generators of the standard Voronoi diagram; something that is in contradistinction with what is the case for the ZVD when the drift is varying uniformly with time [11]. In addition, as illustrated in Fig. 6, we observe that the boundaries of some cells contain the points at which the time-to-go function undergoes discontinuous jumps. Finally, we should also point out that the ZVDs illustrated in Fig. 5 have significantly more complex structure from those presented in earlier attempts to solve similar partitioning problems for constant, temporally and/or spatially varying drift fields [11–14].

6 Conclusion

In this paper, we have characterized the solution of a Voronoi-like partitioning problem which encodes the proximity relations between the members of a team of spatially distributed vehicles and arbitrary points in the plane based on the minimum time-to-go function of the classical Zermelo navigation problem from optimal control theory. Each set of this Voronoi-like partition is uniquely associated with a vehicle such that all points in the set can be reached by the corresponding vehicle faster than any other vehicle from the same team. The partition is constructed by using its interpretation as a forest of cost surfaces emanating from each generator, where the computation of the latter is based on a numerically efficient scheme for the expansion of the level

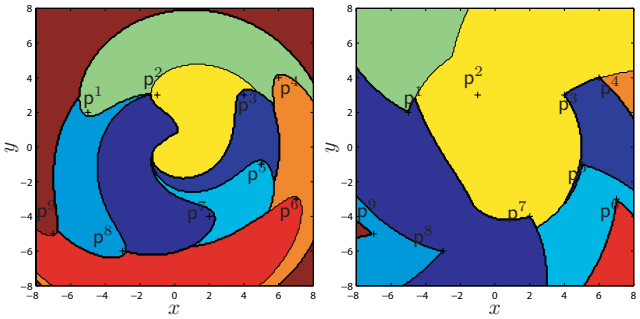

(a) Scenario with time-varying linear drift (b) Scenario with time-invariant linear drift

Fig. 5. The Zermelo-Voronoi diagram generated by a set of nine generators.

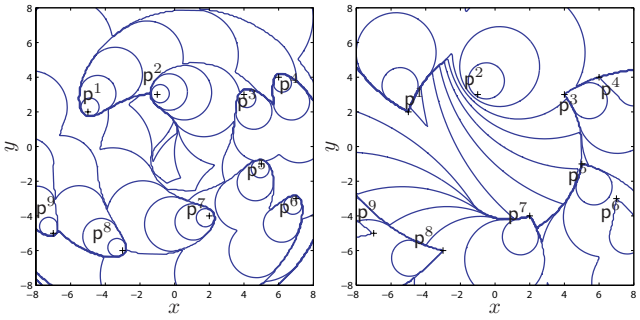

(a) Scenario with time-varying linear drift (b) Scenario with time-invariant linear drift

Fig. 6. Level sets of the minimum time-to-go function emanating from each generator restricted to their corresponding cells.

sets of the minimum time-to-go function. The key advantage of our approach has to do with the fact that the level set expansion scheme exploits the structure of the optimal synthesis of the Zermelo navigation problem. The proposed approach is based on tools and techniques that can be employed to address similar partitioning problems with respect to other state-dependent distance functions. One possible direction for future work would be the design of algorithms for the characterization of the Voronoi-like partition tailored to the topological properties of the partition, when the latter can be established a priori for different classes of drift fields. Another option is to consider variations of the presented partitioning problem that deal with scenarios where the agents do not have a priori global knowledge of the drift field.

Acknowledgements

The authors would like to thank the anonymous reviewers for their constructive comments and suggestions.

References

[1] A. Getis and B. Boots, *Models of Spatial Processes: An Approach to the Study of Point, Line and Area Patterns*. Cambridge, UK: Cambridge University Press, 1978.

[2] D. Ucinski, "Optimal sensor location for parameter estimation of distributed processes," *International Journal of Control*, vol. 73, no. 13, pp. 1235–1248, 2000.

[3] J. Cortés, S. Martinez, T. Karatas, and F. Bullo, "Coverage control for mobile sensing networks," *IEEE Transactions on Robotics and Automation*, vol. 20, no. 2, pp. 243–255, 2004.

[4] J. Cortés and F. Bullo, "Coordination and geometric optimization via distributed dynamical systems," *SIAM Journal of Optimization and Control*, vol. 44, no. 5, pp. 1543–1574, 2005.

[5] S. Martinez, J. Cortés, and F. Bullo, "Motion coordination with distributed information," *IEEE Control Systems Magazine*, vol. 27, no. 4, pp. 75–88, 2007.

[6] F. Bullo, J. Cortés, and S. Martinez, *Distributed Control of Robotic Networks*. Applied Mathematics Series, Princeton, 2009.

[7] M. Schwager, D. Rus, and J. J. E. Slotine, "Adaptation and consensus learning for decentralized coverage control of networked robots," *International Journal of Robotics Research*, vol. 28, no. 2, pp. 357–375, 2009.

[8] A. Kwok, *Deployment Algorithms for Mobile Robots under Dynamic Constraints*. Ph.D. dissertation, Mechanical and Aerospace Engineering, The University of California at San Diego, San Diego, CA, 2011.

[9] S. D. Bopardikar, L. S. Smith, and F. Bullo, "On vehicle placement to intercept moving targets," *Automatica*, vol. 47, no. 9, pp. 2067–2074, 2011.

[10] E. Zermelo, "Über das Navigationproble bei ruhender oder veränderlicher Windverteilung," *Zeitschrift für Angewandte Mathematik und Mechanik*, vol. 11, no. 2, pp. 114–124, 1931.

[11] E. Bakolas and P. Tsiotras, "The Zermelo-Voronoi diagram: a dynamic partition problem," *Automatica*, vol. 46, no. 12, pp. 2059–2067, 2010.

[12] K. Sugihara, "Voronoi diagrams in a river," *International Journal of Computational Geometry and Applications*, vol. 2, no. 1, pp. 29–48, 1992.

[13] T. Nishida, K. Sugihara, and M. Kimura, "Stable marker-particle method for the Voronoi diagram in a flow field," *Journal of Computational and Applied Mathematics*, vol. 202, no. 2, pp. 377–391, 2007.

[14] T. Nishida and T. Sugihara, "Boat-sail Voronoi diagram and its application," *International Journal of Computational Geometry & Applications*, vol. 19, no. 5, pp. 425–440, 2009.

[15] F. Labelle and J. R. Shewchuk, "Anisotropic Voronoi diagrams and guaranteed quality anisotropic mesh generation," in *SCG' 03: Proceedings of the nineteenth annual symposium on Computational Geometry*, pp. 191–200, 2003.

[16] J.-D. Boissonnat, C. Wormser, and M. Yvinec, "Anisotropic diagrams: Labelle Shewchuk approach revisited," *Theoretical Computer Science*, vol. 408, no. 2–3, pp. 163–173, 2008.

[17] F. Aurenhammer, "Voronoi diagrams: A survey of a fundamental geometric data structure," *ACM Computing Surveys*, vol. 23, no. 3, pp. 345–405, 1991.

[18] A. Okabe, B. Boots, K. Sugihara, and S. N. Chiu, *Spatial Tessellations: Concepts and Applications of Voronoi Diagrams*. West Sussex, England: John Wiley and Sons Ltd, second ed., 2000.

[19] R. Klein, "Concrete and abstract Voronoi diagrams," *Lecture Notes in Computer Science*, vol. 400, 1987.

[20] H. Edelsbrunner and S. Seidel, "Voronoi diagrams and arrangements," in *Proceedings of 1st ACM Symp. Computational Geometry*, (Baltimore, MD), pp. 251–262, Jun. 5–7, 1985.

[21] M. Sharir, "Almost tight upper bounds for lower envelopes in higher dimensions," *Discrete & Computational Geometry*, vol. 12, no. 1, pp. 327–345, 1994. doi:10.1007/BF02574384.

[22] J.-D. Boissonnat and M. Yvinec, *Algorithmic Geometry*. Cambridge, United Kingdom: Cambridge University Press, 1998.

[23] K. E. Hoff, III, J. Keyser, M. Lin, D. Manocha, and T. Culver, "Fast computation of generalized Voronoi diagrams using graphics hardware," in *Proceedings of the 26th annual conference on Computer graphics and interactive techniques*, SIGGRAPH '99, (New York, NY, USA), pp. 277–286, 1999.

[24] M. Denny, "Solving geometric optimization problems using graphics hardware," *Computer Graphics Forum*, vol. 22, no. 3, pp. 441–451, 2003.

[25] C. Carathéodory, *Calculus of Variations and Partial Differential Equations of First Order*. Washington DC: American Mathematical Society, third ed., 1999.

[26] V. Jurdjevic, *Geometric Control Theory*. New York: Cambridge University Press, 1997.

[27] A. E. Bryson and Y. C. Ho, *Applied Optimal Control*. Waltham, MA: Blaisdell Publication, 1969.

[28] S. J. Bijlsma, "Optimal aircraft routing in general wind fields," *Journal of Guidance, Control, and Dynamics*, vol. 32, no. 3, pp. 327–345, 2009.

[29] B. Rhoads, I. Mezić, and A. Poje, "Minimum time feedback control of autonomous underwater vehicles," in *Proceedings of 49th IEEE Conference on Decision and Control*, (Atlanta, GA), pp. 5828–5834, December 15–17, 2010.

[30] M. R. Jardin and A. E. Bryson, "Methods for computing minimum-time paths in strong winds," *Journal of Guidance, Control, and Dynamics*, vol. 35, no. 1, pp. 327–345, 2012.

[31] E. Bakolas and P. Tsiotras, "Optimal pursuit of moving targets using dynamic Voronoi diagrams," in *Proceedings of IEEE International Conference on Decision and Control*, (Atlanta, GA), pp. 7431–7436, December 15–17, 2010.

[32] E. Bakolas and P. Tsiotras, "Relay pursuit of a maneuvering target using dynamic Voronoi diagrams," *Automatica*, vol. 48, no. 9, pp. 2213–2220, 2012.

[33] E. D. Sontag, *Mathematical Control Theory: Deterministic Finite Dimensional Systems*. New York, NY: Springer-Verlag, second ed., 1998.

[34] E. B. Lee and L. Markus, *Foundations of Optimal Control Theory*. Malabar, Florida: Krieger Publishing Company, second ed., 1986.

[35] L. D. Berkovitz, *Optimal Control Theory*. New York, NY: Springer-Verlag, 1974.

[36] M. Cesari, *Optimization - Theory and Applications. Problems with Ordinary Differential Equations*. New York: Springer-Verlag, 1983.

[37] J. A. Sethian, *Level Set Methods and Fast Marching Methods*. Cambridge: Cambridge University Press, second ed., 1999.

[38] L. S. Pontryagin, V. G. Boltyaskii, R. V. Gamkrelidze, and E. F. Mishchenko, *The Mathematical Theory of Optimal Processes*. New York: Interscience Publishers, translation from the Russian ed., 1962.

[39] H. Sagan, *Introduction to the Calculus of Variations*. New York: Dover Publications, 1992.

[40] U. Serres, "On the curvature of two-dimensional optimal control systems and Zermelo's navigation problem," *Journal of Mathematical Sciences*, vol. 135, no. 4, pp. 3224–3243, 2006.

[41] E. Bakolas and P. Tsiotras, "Minimum-time paths for a light aircraft in the presence of regionally-varying strong winds," in *AIAA Infotech at Aerospace*, (Atlanta, GA), April 20–22, 2010. AIAA Paper 2010-3380.

[42] S. Willard, *General Topology*. Mineola, NY: Dover, 1998.